Technical Report Documentation Page

1. Report No. FHWA/TX-09/0-5708-2	2. Government Accession No.	3. Recipient's Catalog No.
4. Title and Subtitle Improved Pavement Distress Rating System		5. Report Date August 2008; Rev. October 2008
		6. Performing Organization Code
7. Author(s) Bugao Xu, Ming Yao, Xun Yao, and Quingguang Li		8. Performing Organization Report No. 0-5708-2
9. Performing Organization Name and Address Center for Transportation Research The University of Texas at Austin 3208 Red River, Suite 200 Austin, TX 78705-2650		10. Work Unit No. (TRAIS) 11. Contract or Grant No. 0-5708
12. Sponsoring Agency Name and Address Texas Department of Transportation Research and Technology Implementation Office P.O. Box 5080 Austin, TX 78763-5080		13. Type of Report and Period Covered Technical Report 9/1/07-8/31/08 14. Sponsoring Agency Code
15. Supplementary Notes Project performed in cooperation with the Texas Department of Transportation and the Federal Highway Administration.		
16. Abstract Report to describe the improvements made in hardware and software for pavement cracking detections, and the field test results that show the repeatability, accuracy of the data.		
17. Key Words Crack detection, linear lighting, laser illumination, linescan camera	18. Distribution Statement No restrictions. This document is available to the public through the National Technical Information Service, Springfield, Virginia 22161; www.ntis.gov.	

19. Security Classif. (of report)	20. Security Classif. (of this page)	21. No. of pages	22. Price
Unclassified	Unclassified	46	

Form DOT F 1700.7 (8-72) Reproduction of completed page authorized

IMPROVED PAVEMENT DISTRESS RATING SYSTEM

Bugao Xu
Ming Yao
Xun Yao
Qingguang Li

CTR Technical Report:	0-5708-2
Report Date:	August 2008; Revised October 2008
Project:	0-5708
Project Title:	Improving Capabilities of Automated Distress Rating
Sponsoring Agency:	Texas Department of Transportation
Performing Agency:	Center for Transportation Research at The University of Texas at Austin

Project performed in cooperation with the Texas Department of Transportation and the Federal Highway Administration.

Center for Transportation Research
The University of Texas at Austin
3208 Red River
Austin, TX 78705

www.utexas.edu/research/ctr

Disclaimers

Author's Disclaimer: The contents of this report reflect the views of the authors, who are responsible for the facts and the accuracy of the data presented herein. The contents do not necessarily reflect the official view or policies of the Federal Highway Administration or the Texas Department of Transportation (TxDOT). This report does not constitute a standard, specification, or regulation.

Patent Disclaimer: The University of Texas at Austin filed patent **"Real-Time, High-Speed Pavement Cracking Distress Inspection System"** on May 23, 2006. It is pending.

Notice: The United States Government and the State of Texas do not endorse products or manufacturers. If trade or manufacturers' names appear herein, it is solely because they are considered essential to the object of this report.

Engineering Disclaimer

NOT INTENDED FOR CONSTRUCTION, BIDDING, OR PERMIT PURPOSES.

Research Supervisor: Dr. Bugao Xu

Acknowledgments

The authors express appreciation to Project Director Todd Copenhaver, CST and Project Coordinator Mike Murphy, CST, for their support and advice to the project.

Products

This report contains depictions of the Crackscope (page 3), and VNet (page 4).

Table of Contents

List of Figures

List of Tables

Chapter 1. Purpose and Scope of the Project

The automated pavement distress rating system was developed under the Texas Department of Transportation (TxDOT) research program over the past several years. The system is supposed to scan 100% of the pavement surfaces at any vehicle speed between 5 and 70 miles per hour, detect cracks in real time, and transmit the rating results to the central computer at a specified distance interval (per station or per 0.1 mile). Currently, the system uses high-intensity light emission diode (LED) array as the artificial light source. An array of LEDs is mounted behind a cylindrical lens to form a 0.5-inch-wide beam. The LED emits lights with a narrow band of wavelengths, permitting selective filtering of the sunlight to reduce possible shadows of the vehicle and roadside objects.

However, the LED configuration has its limitations. LEDs are serially connected in a single unit. If one LED is burned due to the high working temperature or current surge, it will cause an open circuit. Further, The LED light bar, mounted on the front bumper of the vehicle, becomes too wide for safe driving when it needs to cover a 12-feet wide pavement.

The objective of this research is to replace the LED light bar with another linear light source which should be stable and uniform in illumination and compact in configuration. Also, the new light source should form a stripe covering the pavement width up to 12 feet at a height of 6 feet or less. The light intensity should give sufficient illumination to overcome the sunlight shadow issue. Along with the change of hardware, the modification of the software, specifically the communication behavior between the software and hardware, is also a part of this project.

Chapter 2. Hardware Modification

2.1 Improvement of Artificial Lighting

Right before the LED bar was applied in the project, a high-power laser line projector was another option for the artificial lighting. However, the limitations of the LED bar exhibited in its current application made us reconsider the laser line projector.

The laser line generator that we use is a Magnum II high power class III laser. With a line generating lens of 80°, it is able to cover 12 feet of pavement when placed at 7.2 feet above the ground. The power of the laser is 4 W and is dangerous enough to cause serious eye injury when one is exposed to the radiation without eye protection.

A proximity sensor is included in the hardware unit. It alarms when an unexpected object—for example, a pedestrian—is detected within a distance of 4 feet to the laser, and it shuts off the laser within a distance of 2 feet. Also, a vehicle speed based laser modulation is implemented in the image capturing software CrackScope. When the vehicle speed drops under a predefined value, probably when the vehicle is approaching a stop sign, the software can also shut off the laser. There is also an interlock switch on the laser controller box which shuts off the laser whenever it is necessary.

2.2 Camera Upgrade

We use a GigE line scan camera to capture pavement images. The camera features a 2K CCD array and provides a GigE interface to communicate with the computer. Frame grabbers are no longer needed.

The computer, which runs the CrackScope, can connect to the camera automatically, as long as there is a camera detected through GigE interface. Camera control commands, such as line rate change or exposure change, are sent to the camera by GigE interface.

The camera provides a software interface for per-pixel coefficient adjustment to allow us to compensate the brightness at non-well-illumination area. This is a very useful feature because the non-uniform illumination is a significant problem with this hardware setup. This problem is mainly because the laser generator is a point light source. Although we can use a line generator lense to convert the laser beam into a line, it is technically difficult to make the energy distributed evenly along the line. Plus, due to the camera lens distortion, the central part of the image may appear brighter than the side parts. The CrackScope software package features a camera calibration procedure which can reduce the effect of non-uniform illumination by setting a unique coefficient to each pixel on the camera CCD with respect to a non-well-illuminated sample picture captured by this camera. Pixels at dark area will receive a high coefficient, while pixels in bright area may receive a low coefficient or even 0.

Chapter 3. Real-Time Data Acquisition and Processing Software

The purpose of the data acquisition software, CrackScope, is to collect, process, and transfer the pavement distress data from a high-performance multi-CPU work station to a central data collection node in the VNET network on the survey vehicle.

The line-scan camera is under the control of CrackScope through GigE interface. Camera control commands, such as line rate change caused by the variation of vehicle speed, and exposure change due to the inconsistency of pavement surface, are sent through GigE interface. An image is transferred to the computer's main memory whenever a frame is done. In the mean time, a system interruption is triggered by the GigE driver to notify the CrackScope that a new image is ready to be processed.

CrackScope applies image processing algorithms on pavement images to identify distress utilizing multi-threading technique. Processing result for each pavement image is buffered until a certain running distance is reached. These buffered results are summarized to generate a formatted data report based on the required data types and communication protocol, and then it is transferred to the nodes in network who request for the data packet.

3.1 Image Processing Algorithm

A lot of effort has been made on the developing and refining of the distress identifying algorithms. The main idea of the algorithm is to divide the image into multiple grids first. Each grid is 8 pixels in width and 8 pixels in height. Based on a currently accepted knowledge that the gray value of a pixel along a black crack's central line appears to be darker than the average of background gray value (this rule is also true when applied on white cracks but with the gray value of that pixel being brighter than background average), a detailed grayscale analysis is applied on each grid to determine if this grid contains such a black pixel, which is referred to as a seed pixel. Orientation of a seed can be calculated by examining the grayscale of its neighbor pixels. Cracks are identified by linking all consecutive seed pixels with similar orientations.

3.2 Performance of the Algorithm

According to the basic assumption that crack should be darker than background, the image processing algorithm has been fine tuned to detect cracks under reasonable contrast (picture quality). However, the quality of the picture varies when the illumination condition and pavement surface condition changes, which actually happened a lot when we were doing the field test.

Figure 3.1 and Figure 3.2 show sample pictures we captured on Bull Creek Road South bound. The pictures were taken on a normal sunny afternoon. There was a shower in that morning so that the pavement was flushed and was clean (no dust in the crack). Both of the longitudinal and transverse cracks in the picture are easy to be discerned by visual inspection. Our algorithm has been proved to be capable of detecting cracks as

long as the cracks presented in the picture exhibits similar characteristics as was assumed before.

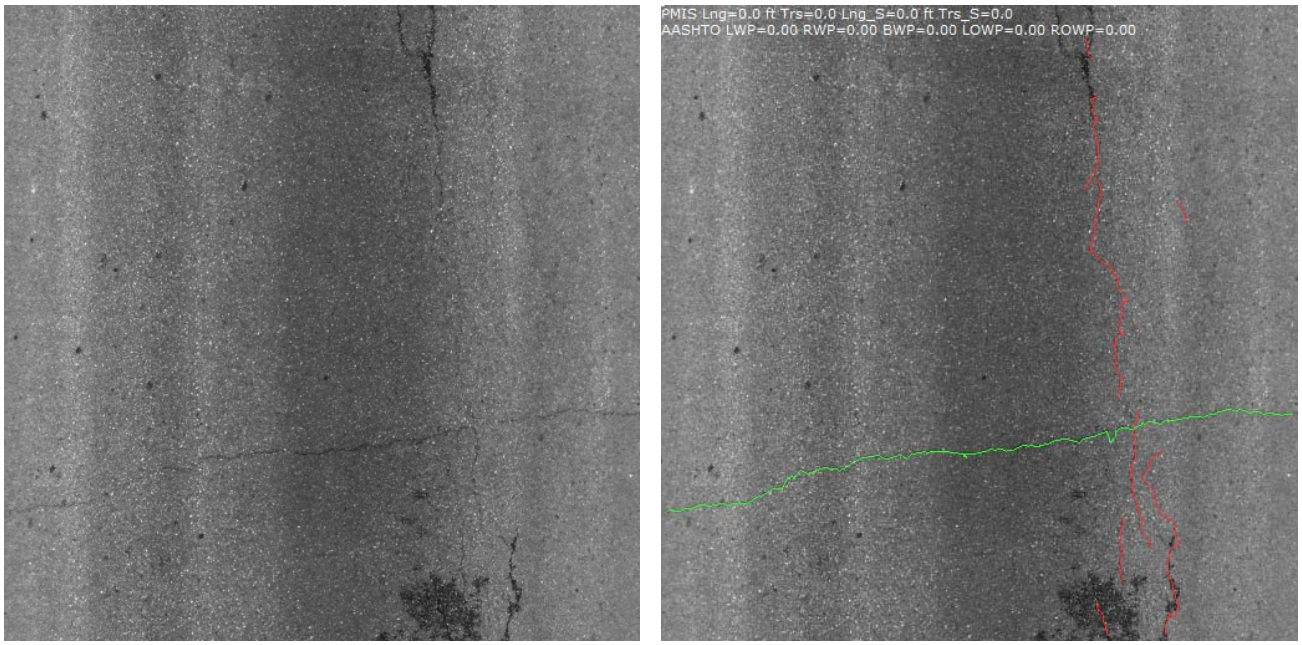

(a) Pavement image taken on Bull Creek Road.

(b) Both of the longitudinal and transverse cracks are detected.

Figure 3.1: Performance of image processing algorithm

Figure 3.3 shows a picture which we would not consider a good sample. This picture was also taken on Bull Creek Road but was on North bound. Although it was well focused and the illumination is uniform, cracks in this picture are not as discernable as those shown in Figure 3.1 and Figure 3.2. This is because these cracks are not wide and deep enough to produce sufficient contrasts since the laser beam is projected vertically perpendicular to the pavement. Besides, on some pavements dust may be deposited and filled in the cracks, making the cracked regions appear whiter than the pavement surface. Currently (by the end of August, 2008), the algorithms cannot reliably detect “white” or “shallow” cracks.

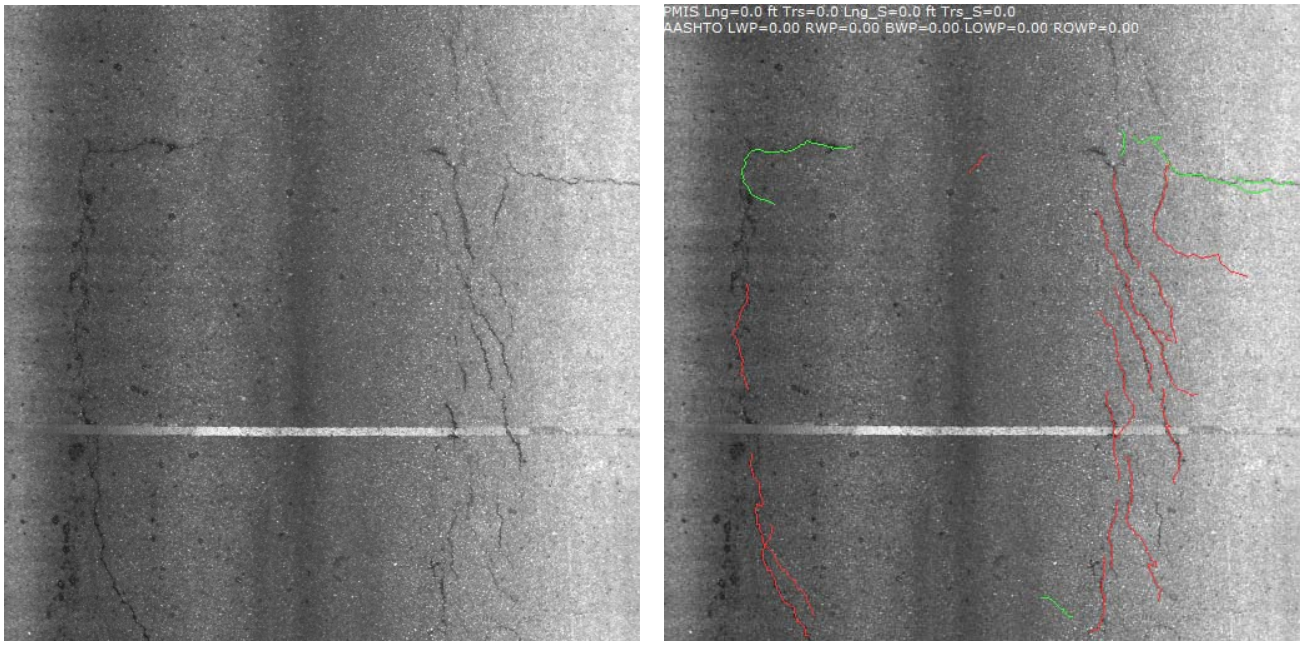

(a) Pavement image taken on Bull Creek Road

(b) Longitudinal and transverse cracks are detected

Figure 3.2: Performance of image processing algorithm

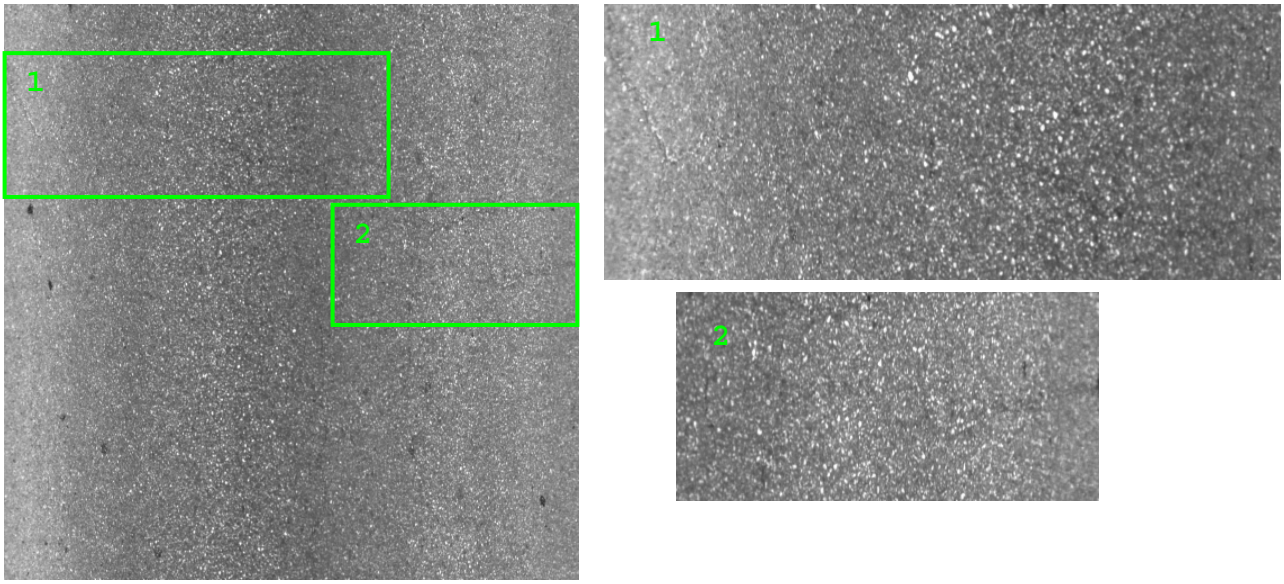

Figure 3.3: Cracks that cannot be detected by our algorithm.

3.3 Survey Data Report

Crack statistic data is reported in compliance with the communication protocol defined by TxDOT. CrackScope only sends data to other modules in the on-vehicle

network which keep active TCP connections with CrackScope. Data is transferred in clear text and are sent every 0.1 mile.

Chapter 4. Field Test Results

Field tests have been made on Bull Creek Road with real traffic to validate the hardware setup, inter-node communication within the on-vehicle network, and the image processing algorithm.

In the current phase, the functions of camera control and image capture have been proven to work. However, the picture quality cannot always be guaranteed. Because the laser beam is focused to be very narrow in order to concentrate its energy, it requires the camera's view area to be accurately aligned with the laser beam. Since vibration on the vehicle is not avoidable, the system needs to be re-aligned regularly, and the flat field correction is recommended to be performed every time the system is powered up.

The illumination issue and the inconsistency condition of pavement pose a great challenge to the image processing algorithm. We have fine tuned the algorithm to improve its accuracy and generalization ability. The generalization ability is a very important part in this application. It is the ability to work with images taken on different types of pavement under inconsistent illumination condition. For example, newly paved vs. long term worn, or clean vs. dusty.

The preciseness of crack detection is verified by comparing automatic detection result with the manual crack map on a section of 1600 feet of pavement of Bull Creek Road northbound. The crack map of automatic crack detection is included in the Appendix A and the crack data is listed in Table 4.1. Compared with the manual crack map, the automatically detected crack map does reflect the positions of cracks actually exist on the pavement. This proves that the chance of the crack detection algorithm to generate false response is very low. However, this is not good enough to demonstrate its effectiveness because the algorithm seems to under-estimate the result. There are still some cracks on the pavement that were missed in the detection result, either because they are not discernable in the picture, or because the algorithm is not robust enough to discover them.

Table 4.1: Crack detection result. Visual rating vs. automatic rating.

	Visual Rating		Automatic Rating	
	Longitudinal Cracking	Transverse Cracks	Longitudinal Cracking	Transverse Cracks
0 - 100	226	14.5	152	5
100 - 200	90	10.5	55	5.5
200 - 300	45	9.5	23	5.5
300 - 400	70	10	14	4
400 - 500	26	11.5	28	8.5
500 - 528	25	3.5	21	4
Total	**482**	**59.5**	**293**	**32.5**
Rating	**91**	**11**		
528 - 600	14	5.5	3	2.5
600 - 700	51	6	42	5.5
700 - 800	60	8	39	7
800 - 900	81	9.5	80	10
900 - 1000	125	8	123	6
1000 - 1056	44	5	27	3
Total	**375**	**42**	**314**	**34**
Rating	**71**	**8**		
1056 - 1100	29	3	5	2
1100 - 1200	56	6	27	4
1200 - 1300	47	3	49	2
1300 - 1400	43	5.5	35	3.5
1400 - 1500	76	5.5	58	3.5
1500 1584	59	5.5	77	2
Total	**310**	**28.5**	**251**	**17**
Rating	**59**	**5**		

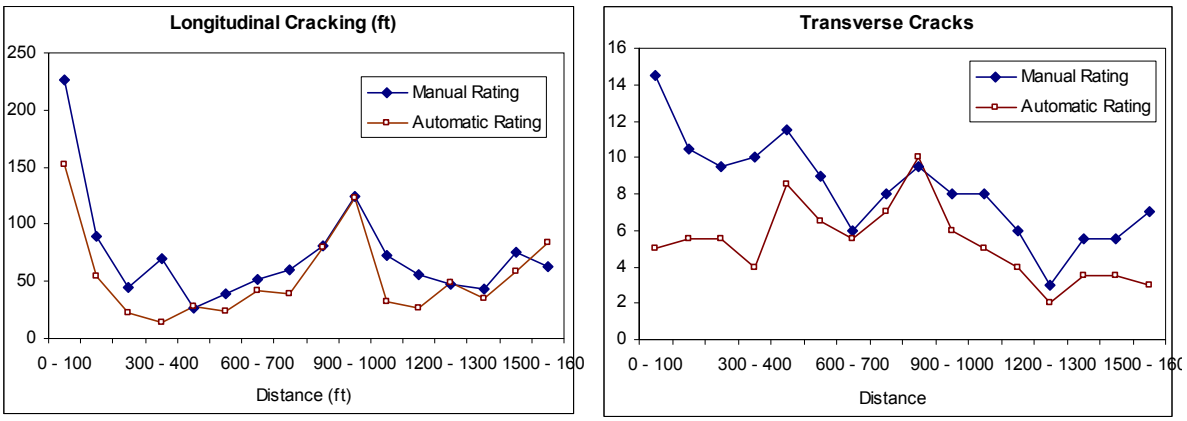

Figure 4.1: Comparison of crack detection result. Manual rating vs. automatic rating.

Repeatability is also a major concern in this application. We performed the repeatability test by scanning the same pavement for several times on different days, and compared the statistic results with each other. The tables and figures listed below are the summary of three field tests we made on Bull Creek Road southbound on April 23, May 6, and June 11, respectively.

Table 4.2: Statistic of longitudinal and transverse cracks for 5 scans made on 04/23/2008

Longidutinal Cracks (unit: ft)								
	0.1 mi	0.2 mi	0.3 mi	0.4 mi	0.5 mi	0.6 mi	0.7 mi	Total
average	54.89	105.02	68.79	65.74	57.44	100.22	106.50	558.60
std	7.33	10.77	7.22	10.59	10.81	9.63	8.04	12.49
cv	0.13	0.10	0.11	0.16	0.19	0.10	0.08	0.02

Transverse Cracks (unit: count)								
	0.1 mi	0.2 mi	0.3 mi	0.4 mi	0.5 mi	0.6 mi	0.7 mi	Total
average	11.78	13.49	13.42	13.46	7.05	5.76	6.05	71.01
std	1.39	0.72	1.03	1.55	0.95	0.73	0.79	2.92
cv	0.12	0.05	0.08	0.11	0.13	0.13	0.13	0.04

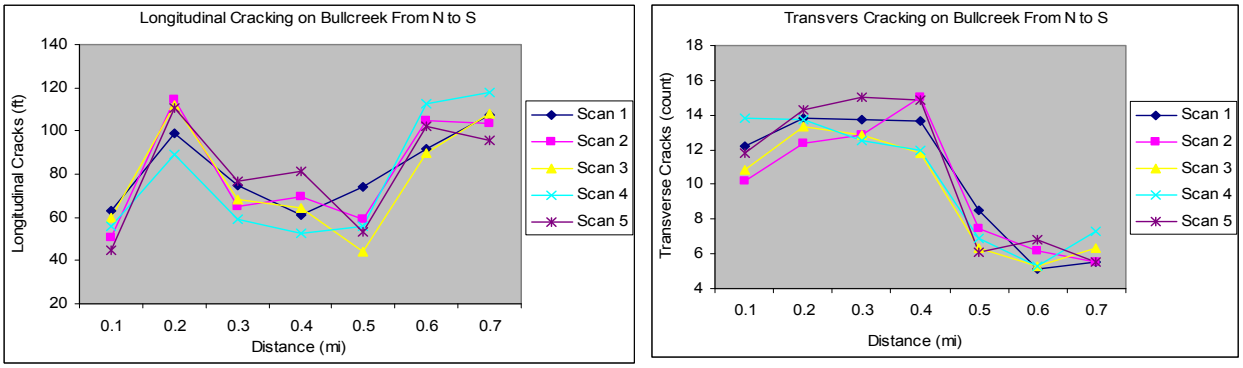

Figure 4.2: Summary of longitudinal and transverse cracks at an interval of 0.1 mile.

Table 4.3: Statistic of longitudinal and transverse cracks for 5 scans made on 05/06/2008

Longidutinal Cracks (unit: ft)								
	0.1 mi	0.2 mi	0.3 mi	0.4 mi	0.5 mi	0.6 mi	0.7 mi	Total
average	63.50	108.08	71.18	69.47	68.11	109.22	107.11	596.67
std	8.02	12.10	5.01	4.24	8.28	2.33	8.98	13.67
cv	0.13	0.11	0.07	0.06	0.12	0.02	0.08	0.02

Transverse Cracks (unit: count)								
	0.1 mi	0.2 mi	0.3 mi	0.4 mi	0.5 mi	0.6 mi	0.7 mi	Total
average	12.81	14.65	14.35	14.90	8.03	6.27	5.30	76.31
std	0.35	0.61	1.20	0.31	0.74	0.35	0.46	0.78
cv	0.03	0.04	0.08	0.02	0.09	0.06	0.09	0.01

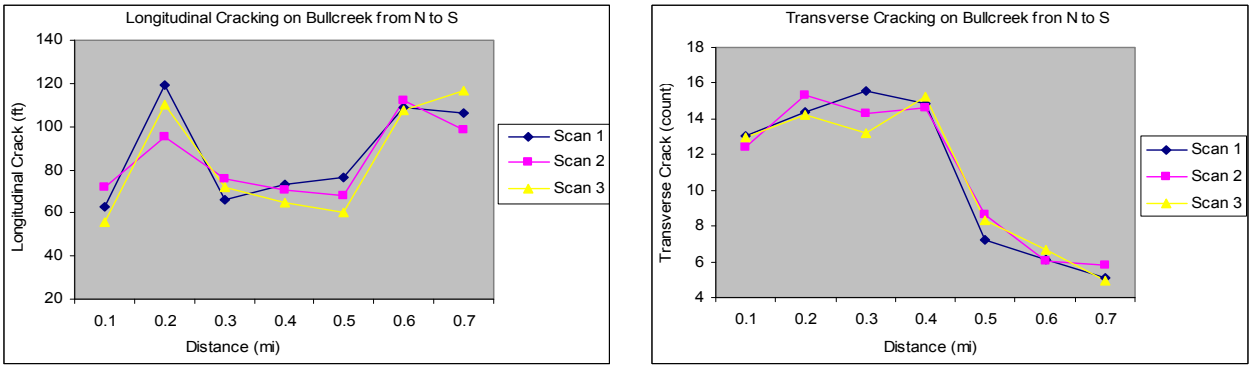

Figure 4.3: Summary of longitudinal and transverse cracks at an interval of 0.1 mile

Table 4.4: Statistic of longitudinal and transverse cracks for 5 scans made on 06/11/2008

Longidutinal Cracks (unit: ft)								
	0.1 mi	0.2 mi	0.3 mi	0.4 mi	0.5 mi	0.6 mi	0.7 mi	Total
average	64.77	111.20	76.59	79.95	75.28	120.54	109.05	637.38
std	5.65	10.66	6.04	7.33	5.68	8.94	11.83	15.91
cv	0.09	0.10	0.08	0.09	0.08	0.07	0.11	0.02

Transverse Cracks (unit: count)								
	0.1 mi	0.2 mi	0.3 mi	0.4 mi	0.5 mi	0.6 mi	0.7 mi	Total
average	11.36	13.90	14.12	13.91	7.99	6.08	6.10	73.47
std	0.96	0.69	0.54	0.69	0.85	0.56	0.54	0.96
cv	0.08	0.05	0.04	0.05	0.11	0.09	0.09	0.01

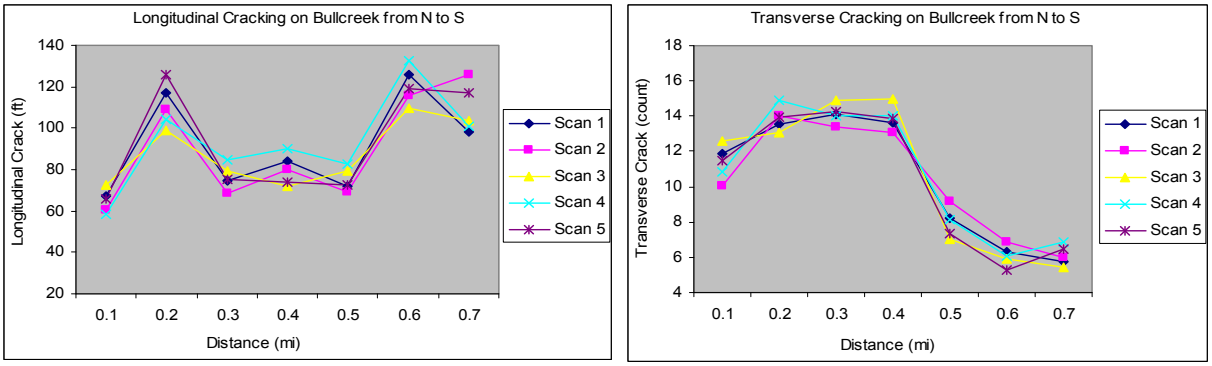

Figure 4.4: Summary of longitudinal and transverse cracks at an interval of 0.1 mile

Table 4.5: Average cracking on different days

	0.1 mi	0.2 mi	0.3 mi	0.4 mi	0.5 mi	0.6 mi	0.7 mi	Total
4/23/2008	54.89	105.02	68.79	65.74	57.44	100.22	106.50	558.60
5/6/2008	63.50	108.08	71.18	69.47	68.11	109.22	107.11	596.67
6/11/2008	64.77	111.20	76.59	79.95	75.28	120.54	109.05	637.38
average	**61.06**	**108.10**	**72.19**	**71.72**	**66.94**	**110.00**	**107.56**	**597.55**
std	**5.38**	**3.09**	**4.00**	**7.36**	**8.98**	**10.18**	**1.33**	**39.39**
cv	**0.09**	**0.03**	**0.06**	**0.10**	**0.13**	**0.09**	**0.01**	**0.07**

	0.1 mi	0.2 mi	0.3 mi	0.4 mi	0.5 mi	0.6 mi	0.7 mi	Total
4/23/2008	11.78	13.49	13.42	13.46	7.05	5.76	6.05	71.01
5/6/2008	12.81	14.65	14.35	14.90	8.03	6.27	5.30	76.31
6/11/2008	11.36	13.90	14.12	13.91	7.99	6.08	6.10	73.47
average	**11.98**	**14.02**	**13.96**	**14.09**	**7.69**	**6.04**	**5.82**	**73.60**
std	**0.75**	**0.59**	**0.49**	**0.73**	**0.55**	**0.26**	**0.45**	**2.65**
cv	**0.06**	**0.04**	**0.03**	**0.05**	**0.07**	**0.04**	**0.08**	**0.04**

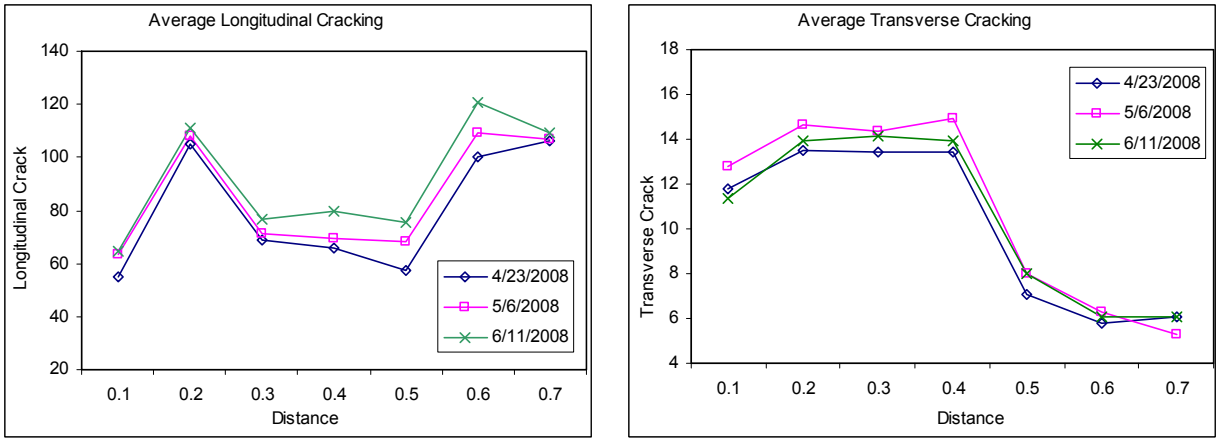

Figure 4.5: Summary of average cracks calculated on different days.

The average results for all field tests are given in Table 4.5 and Figure 4.5. The results show that a roughly 5% to 13% of the coefficient of variation could be expected from the results that are generated by the crack detection algorithm. These results indicate that the performance of the system may not be convincing because the system tends to underestimate the cracking, although the chances that the software reports the existence of cracks that actually do not exist on the road are very low.

Chapter 5. Conclusion

We have developed and tested a new version of a field prototype for a laser-based, real-time detection system for measuring pavement distress as an improvement of capabilities to the automated pavement distress rating system that have been implemented in TxDOT. It achieved the goals of scanning 12-ft wide pavements, covering entire travel distance, and saving and analyzing images at real-time up to 30 mph survey speed. The shadow effect is no longer a problem with the new system. The power consumption is reduced to under 150w.

The test results verified that the principle of our detection system is technically sound and indicated that the algorithm implemented in the software works effectively in most cases. However, when compared with manual crack rating, the image processing algorithm tends to underestimate cracks. This is partly because some of the cracks are not discernable in the picture due to the limited pixel resolution and contrast. Changing the pixel coefficients may improve the overall brightness of captured pictures, but it may not help increase the signal-to-noise ratio. The algorithm also has limited generalization when processing pavements of various textures.

The real-time processing speed can be improved by using more powerful computers and enhancing the efficiency of software coding.

Chapter 6. Further Thoughts

6.1 Increase pixel resolution

In those pictures captured by the current prototype, some narrow and light cracks may not be visible to the human eye, or be detectable by the image processing algorithm. According to its optical configuration, the camera is supposed to cover 12 feet of the pavement. With the width of the image being 2048 pixels, the size of a single pixel is calculated by:

$$pixel\_size = \frac{12(ft) \times 12(in/ft) \times 25.4(mm/in)}{2048} = 1.79mm.$$

However, the basic idea of the crack detection algorithm is to find the darkest pixels in the transverse direction of a crack and then link these pixels together. For this reason, if the width of a crack is less than 3 pixels, the detection algorithm may not work well on that crack. Therefore, if the width of a crack is less than 5.4 (1.8 x 3) mm, it will be difficult to be detected in the picture. We have done some experiments to lower the camera so that it covers 6 feet of the pavement, and ultimately doubles the pixel resolution (Figure 6.1). The quality of pictures taken under this resolution is greatly improved.

One solution is to use a higher resolution camera, say a 4k line-scan camera, to improve the image quality. But a 4K camera normally has lower line rates that prevent real-time, highway speed survey. Another solution is to use two synchronized 2k cameras, each covering half of the lane. This configuration requires a special external circuit to synchronize both cameras, for example, to trigger the capture simultaneously.

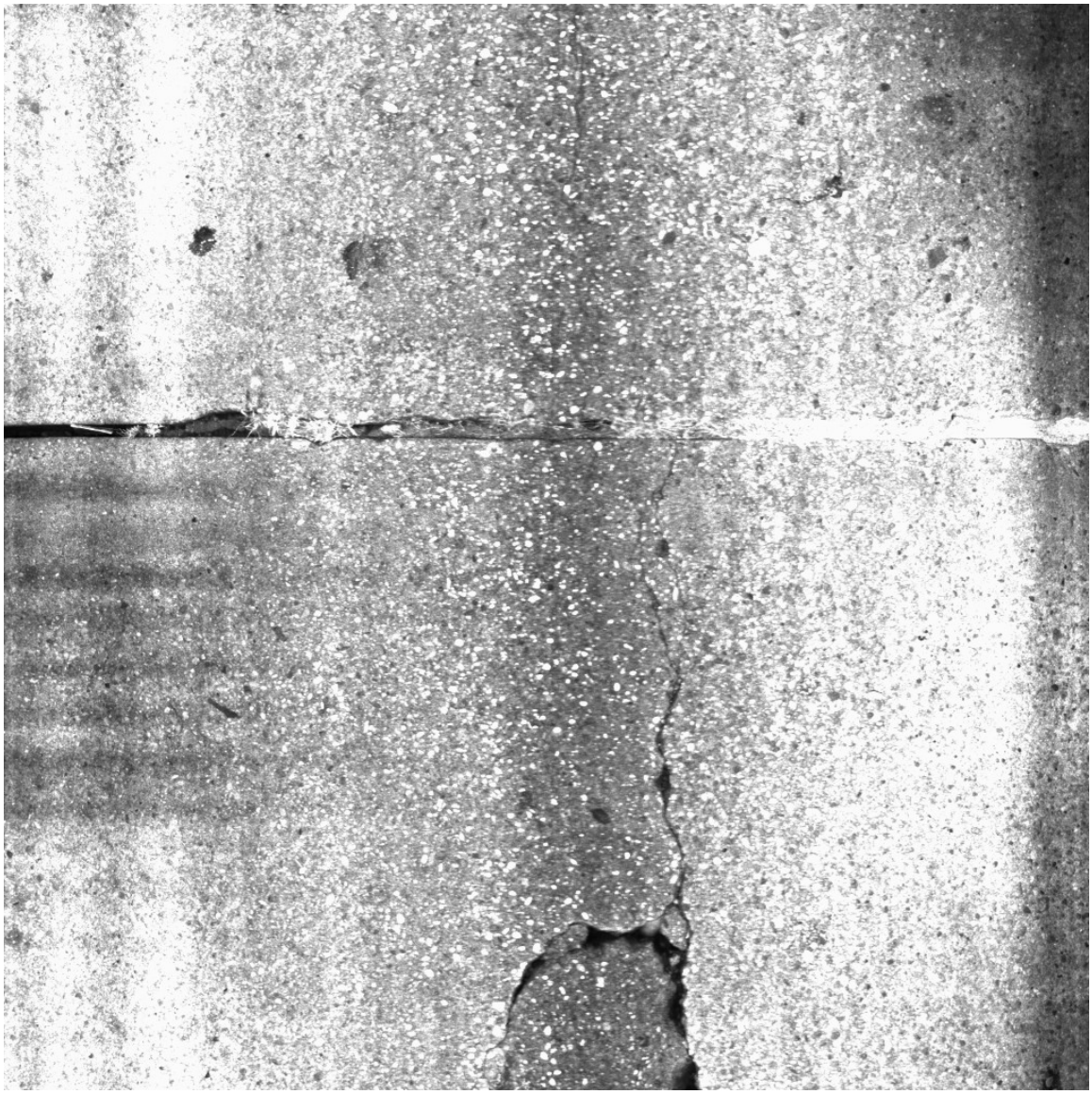

Figure 6.1: Sample picture captured by low-mount camera.

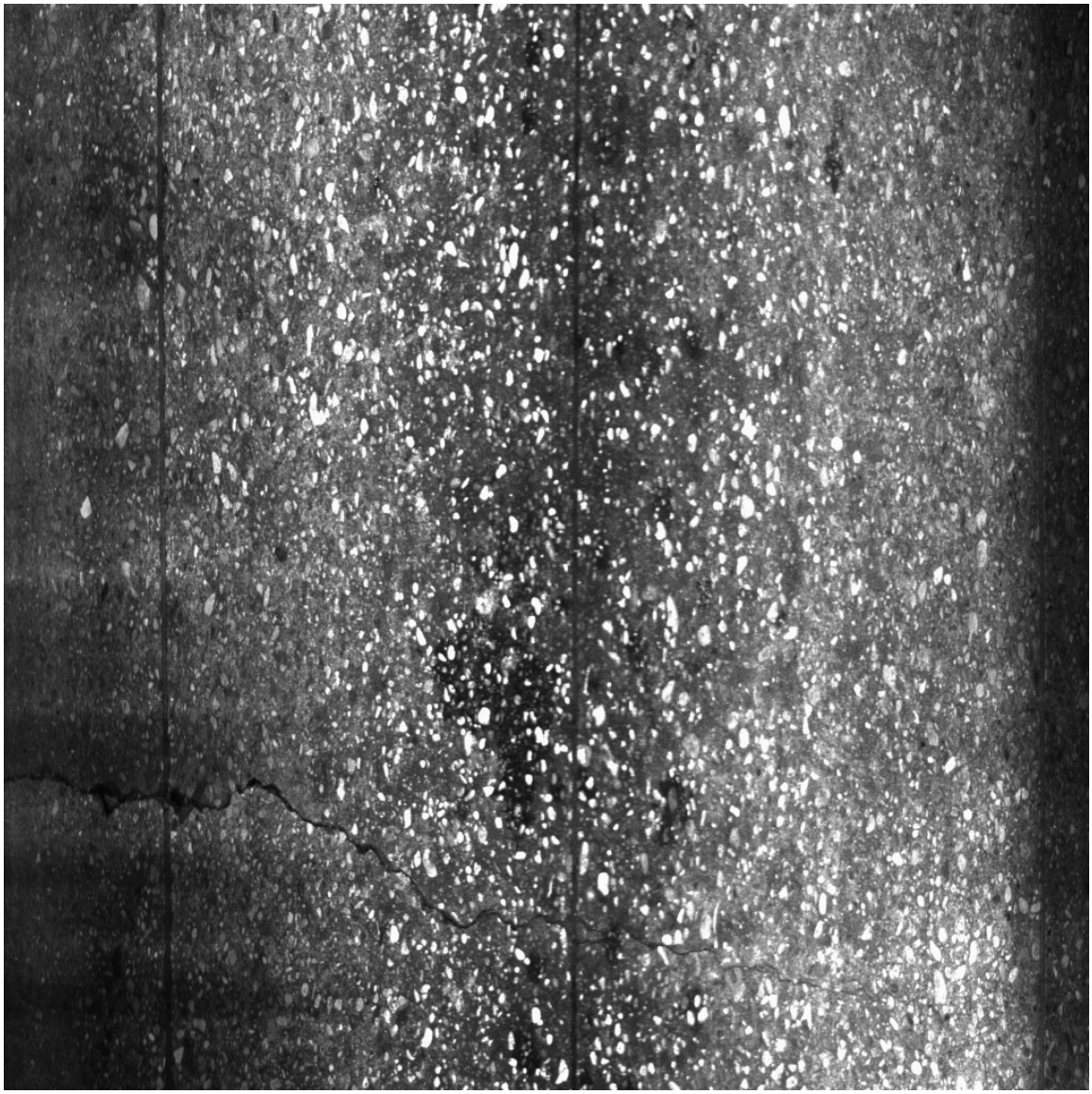

Figure 6.2: Sample picture captured by low-mount camera

6.2 Improve software robustness

The data accuracy is the main bottleneck of the crack detection software. The algorithm is very likely to underestimate the cracks either because the cracks in the picture are not discernable, or because the software is not capable of detecting the cracks with very low contrast or the background of the pavement is highly textured, which is very common in our field test. To improve the generalization ability of the detection algorithm, a lot of new rules need to be introduced in the algorithm framework. For

example, the algorithm should adjust its thresholds when the complexity of the background changes, or the algorithm should lower the standard of identifying a crack if the previous pictures indicate that we are currently in a crack-heavy section. Each of the rules completes the structure of the algorithm more or less, making the algorithm less efficient (slow in processing and hard to maintain).

The crack detection algorithm needs to be revised. But before the modification of the algorithm, an in-deep study of crack characteristics is recommended to capture main features which distinguish a crack from the pavement (background). A reimplementation of the algorithm is preferable because the current software may not meet the requirement of highway speed, real-time image processing.

Appendix A

A.1 Crack Map of Automated Crack Detection

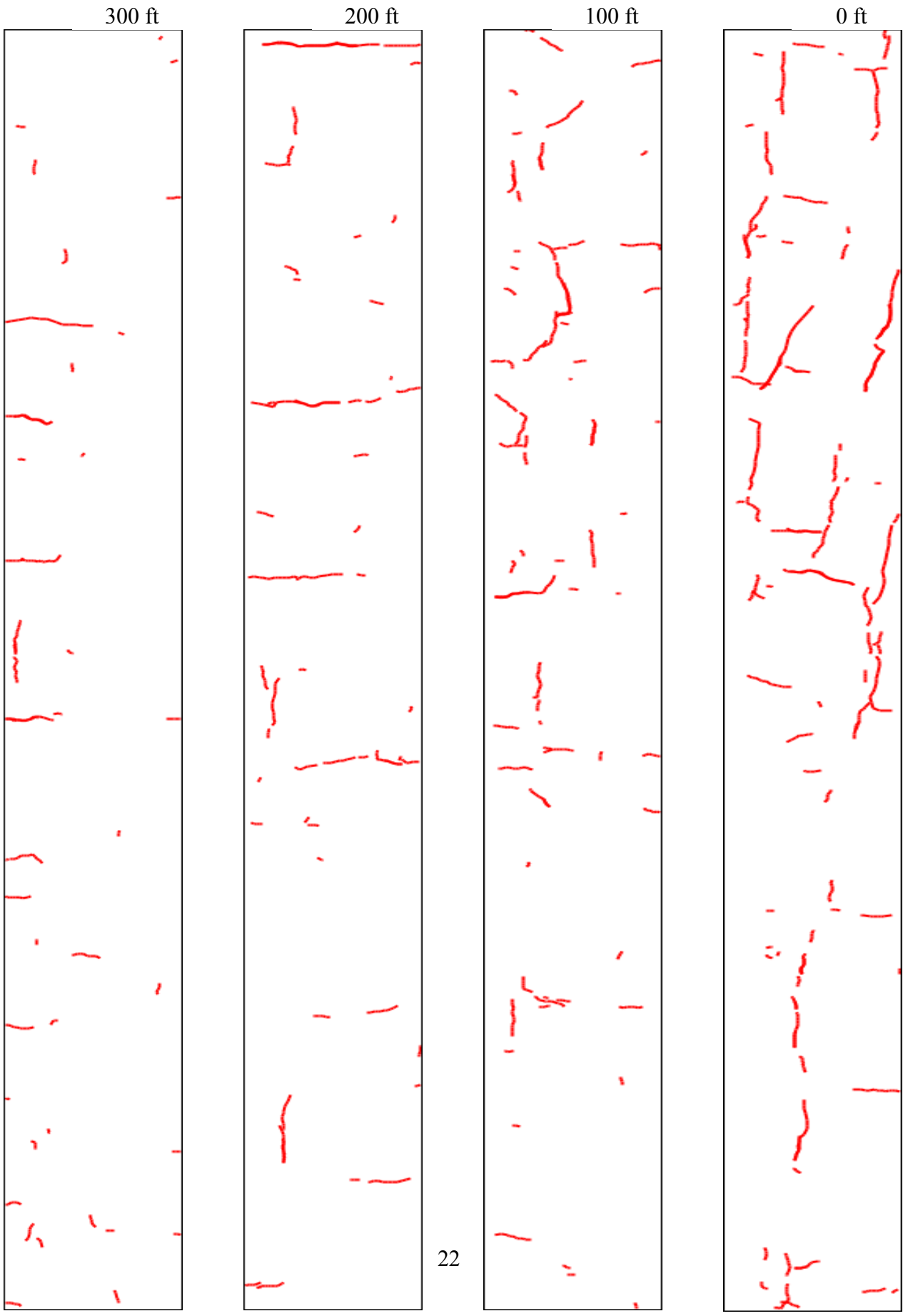
300 ft
200 ft
100 ft
0 ft
Driving direction

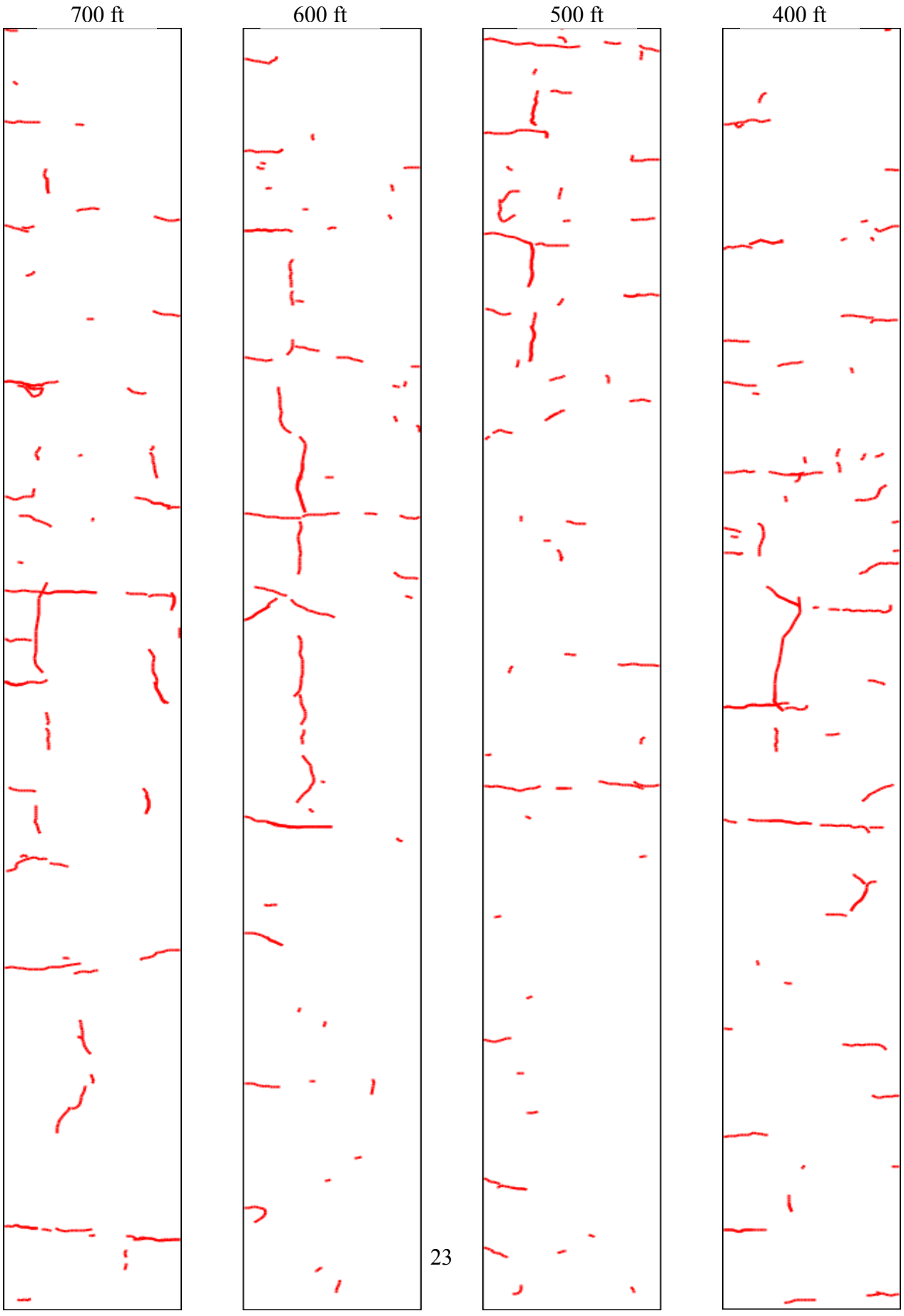
700 ft
600 ft
500 ft
400 ft

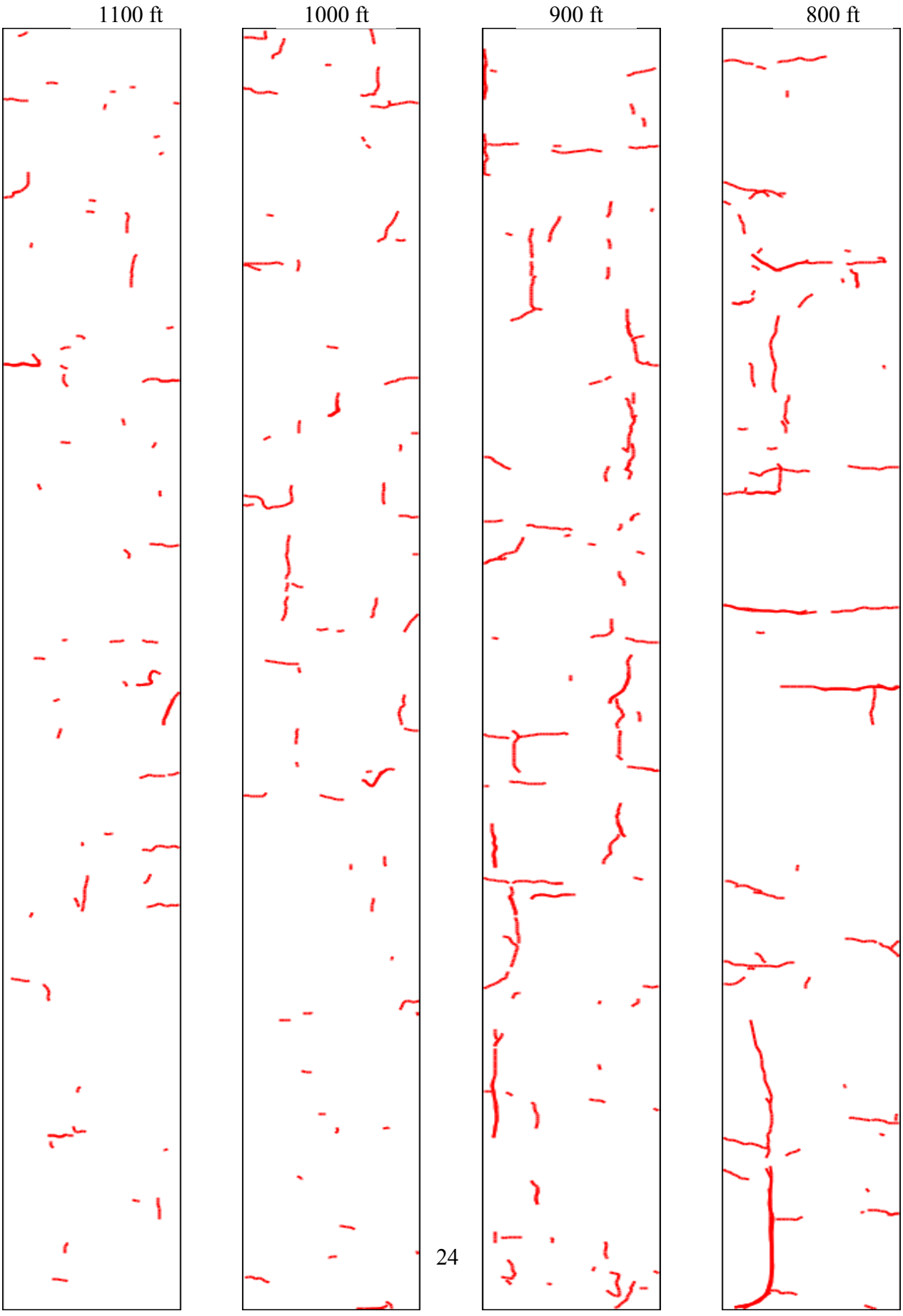
1100 ft
1000 ft
900 ft
800 ft

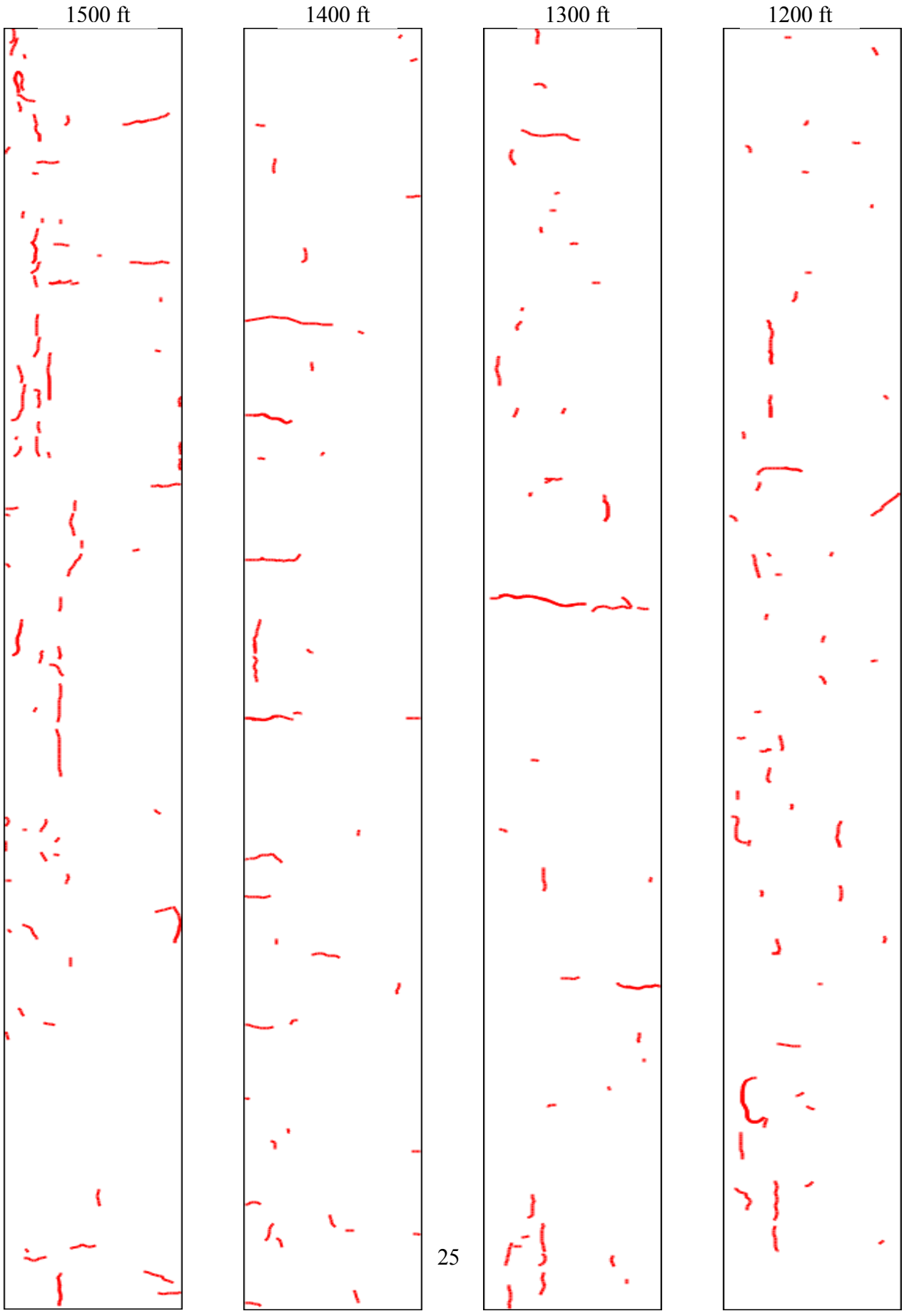
1500 ft
1400 ft
1300 ft
1200 ft

A.2 Crack Detection Results

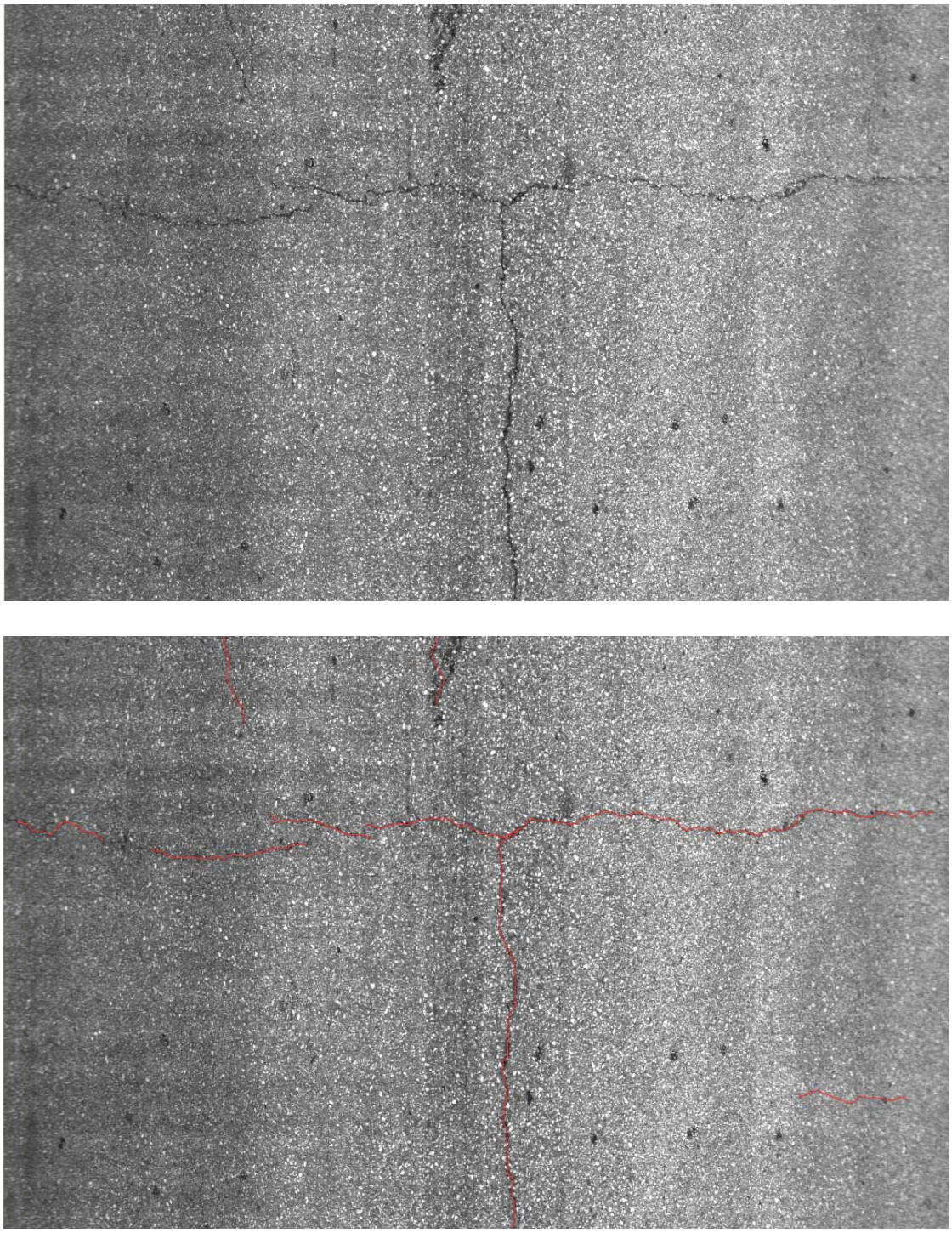

Flexible cracking

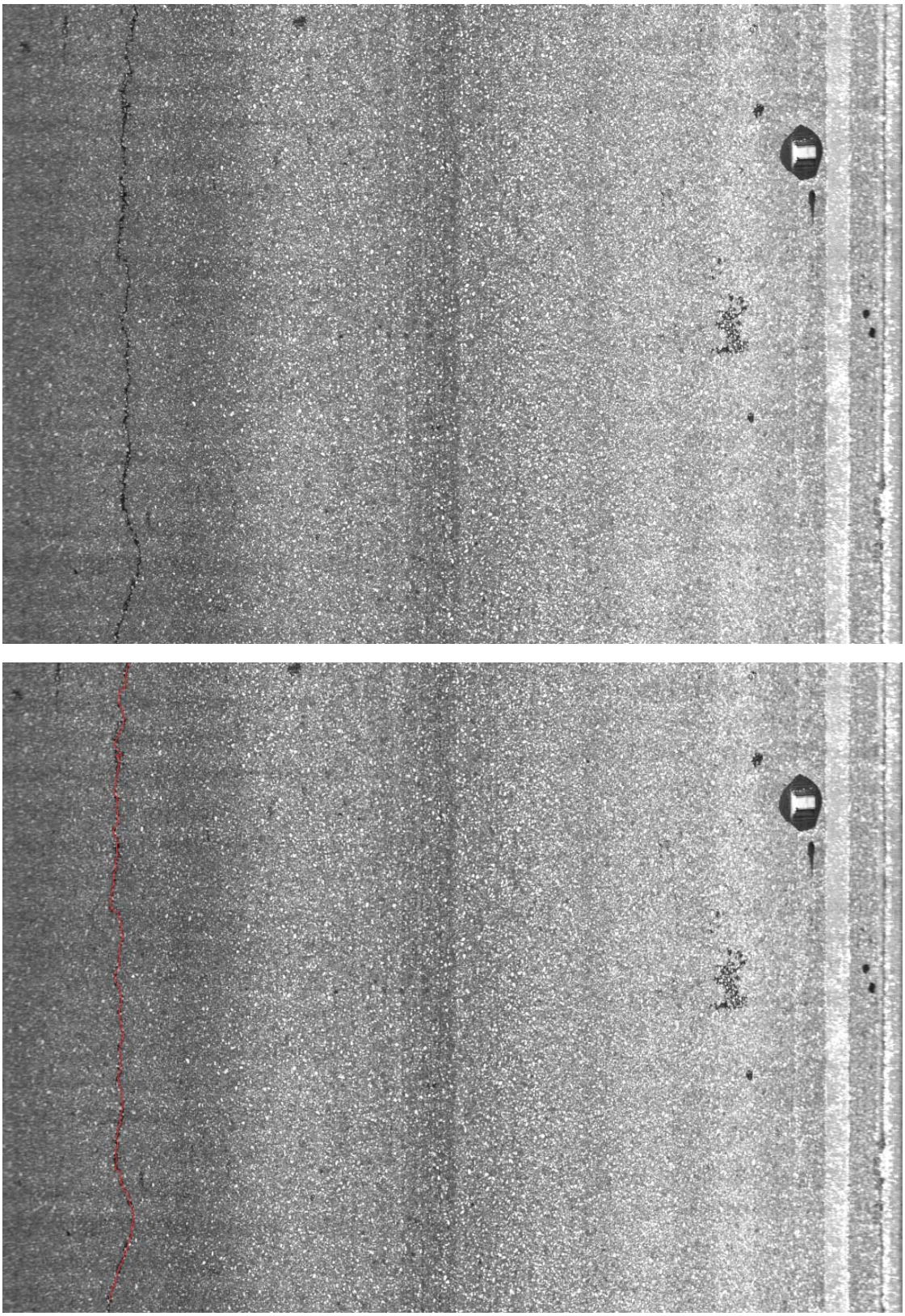

Longitudinal crack

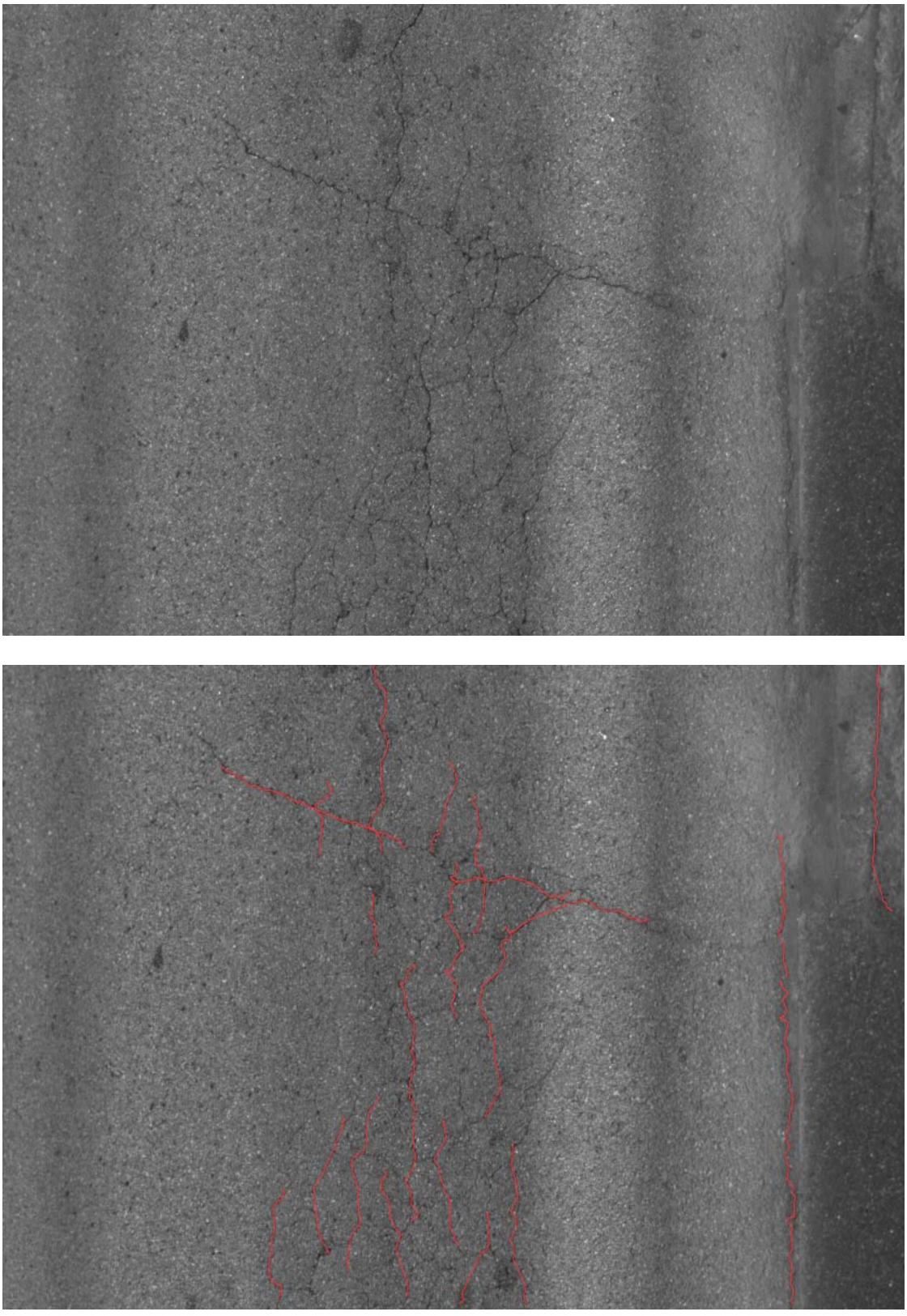

Alligator cracking

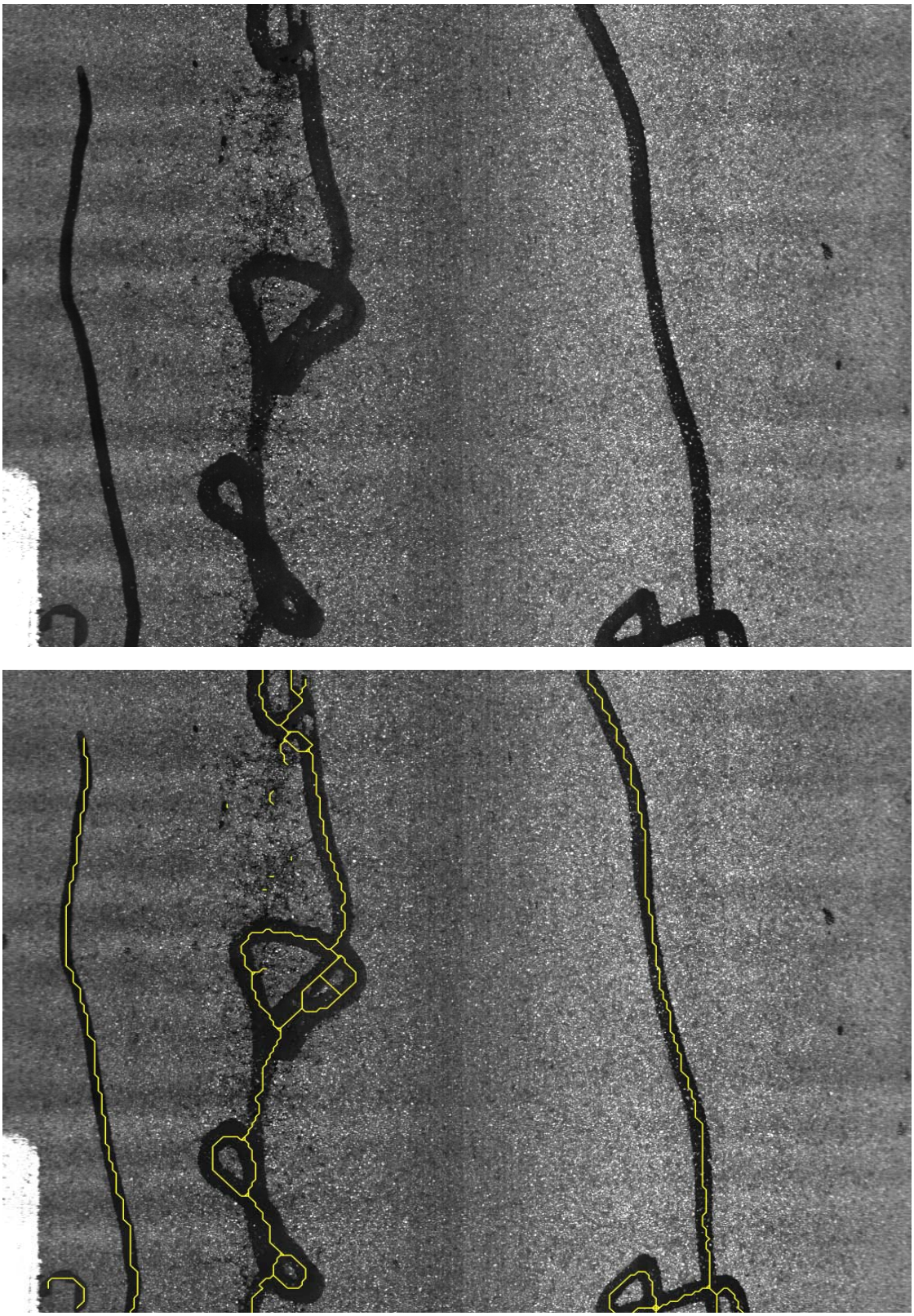

Sealed cracks

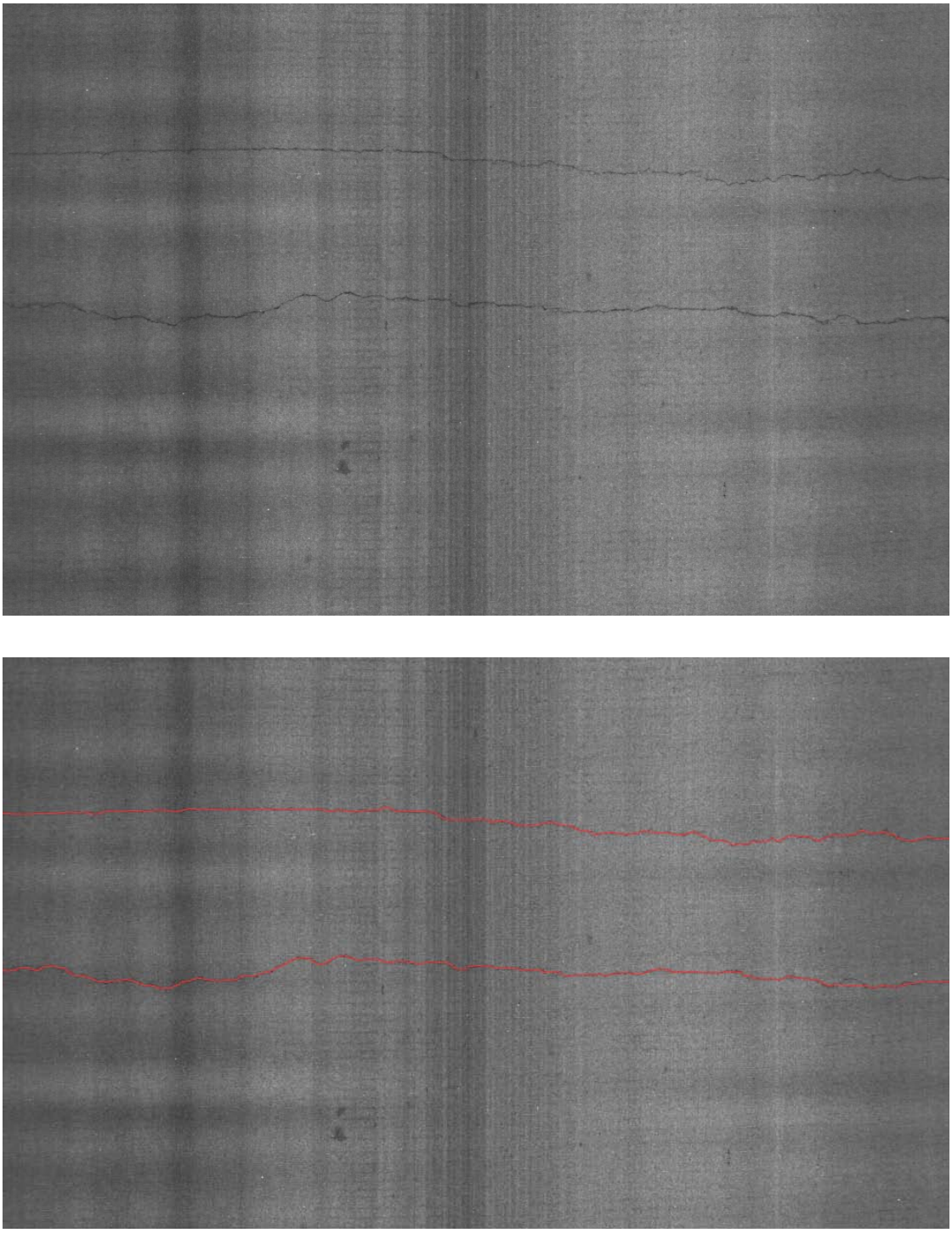

Concrete transverse cracks

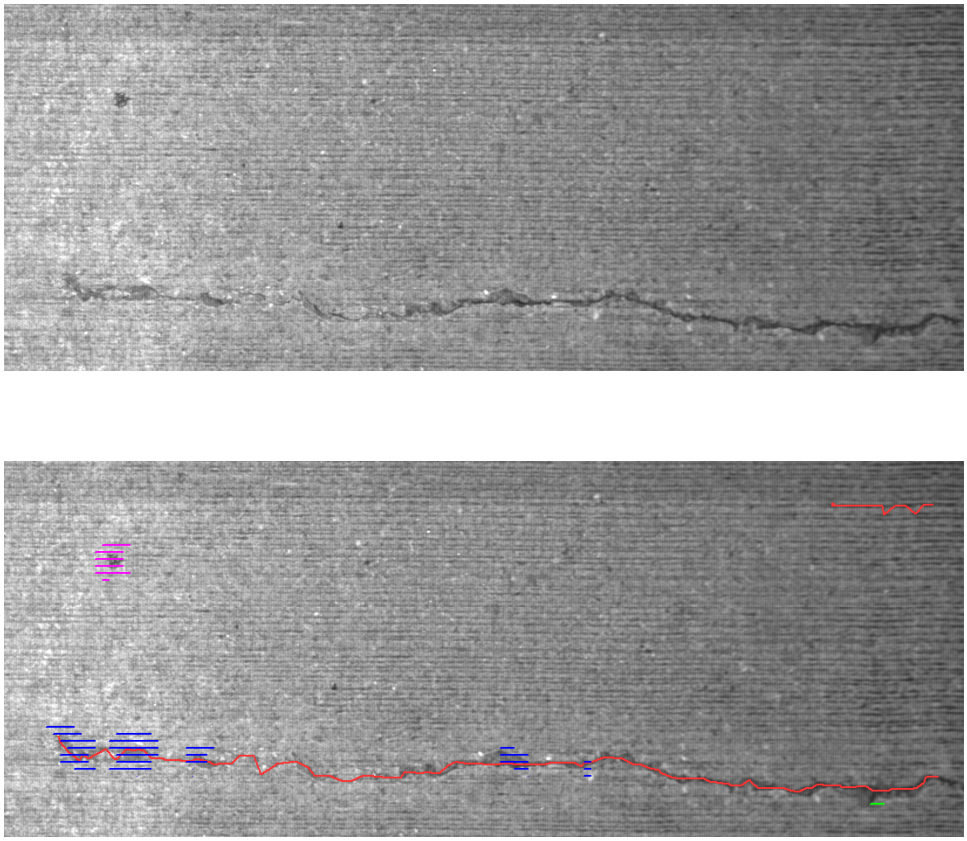

Concrete spalled cracks

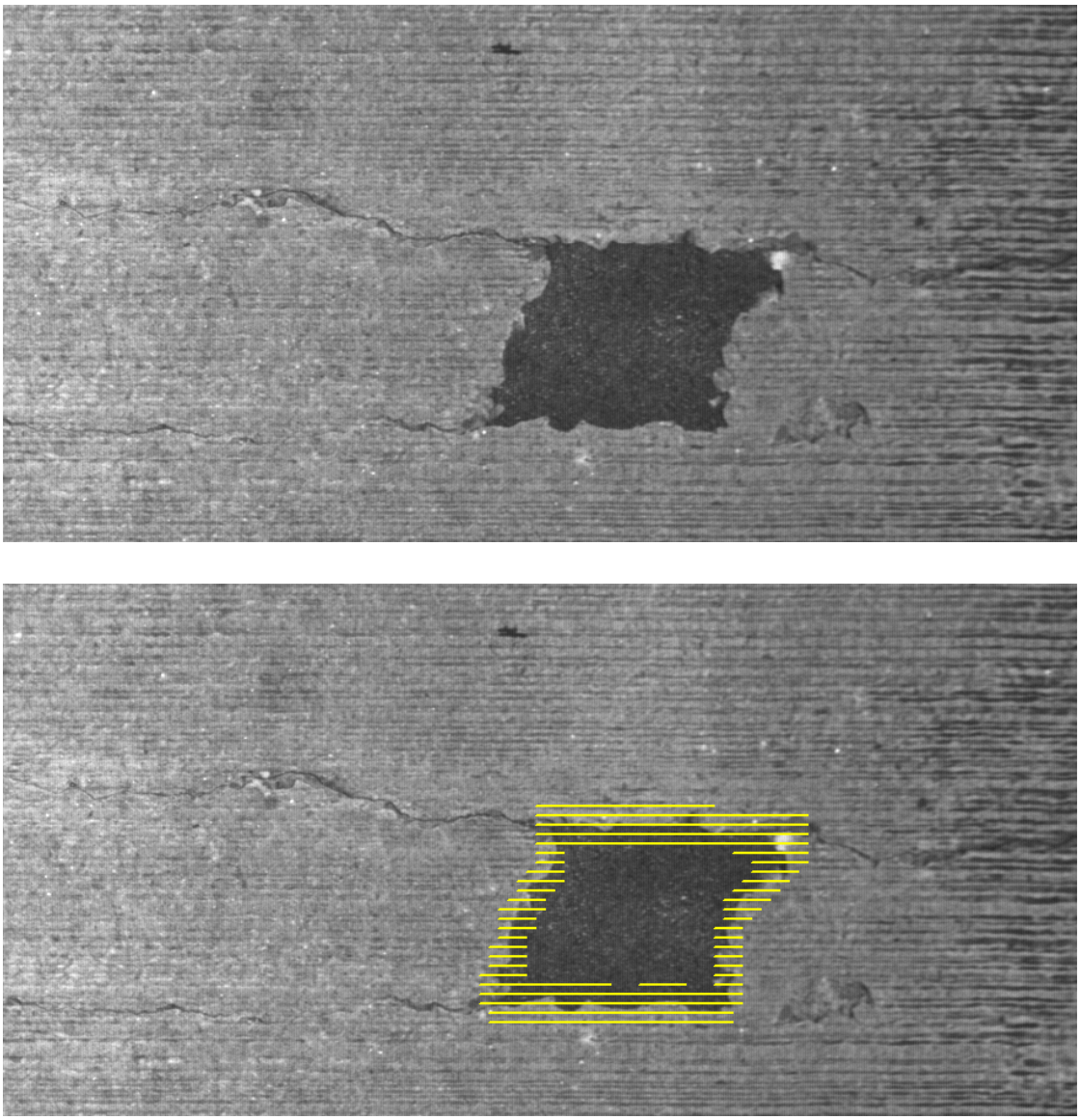

Concrete patch crack

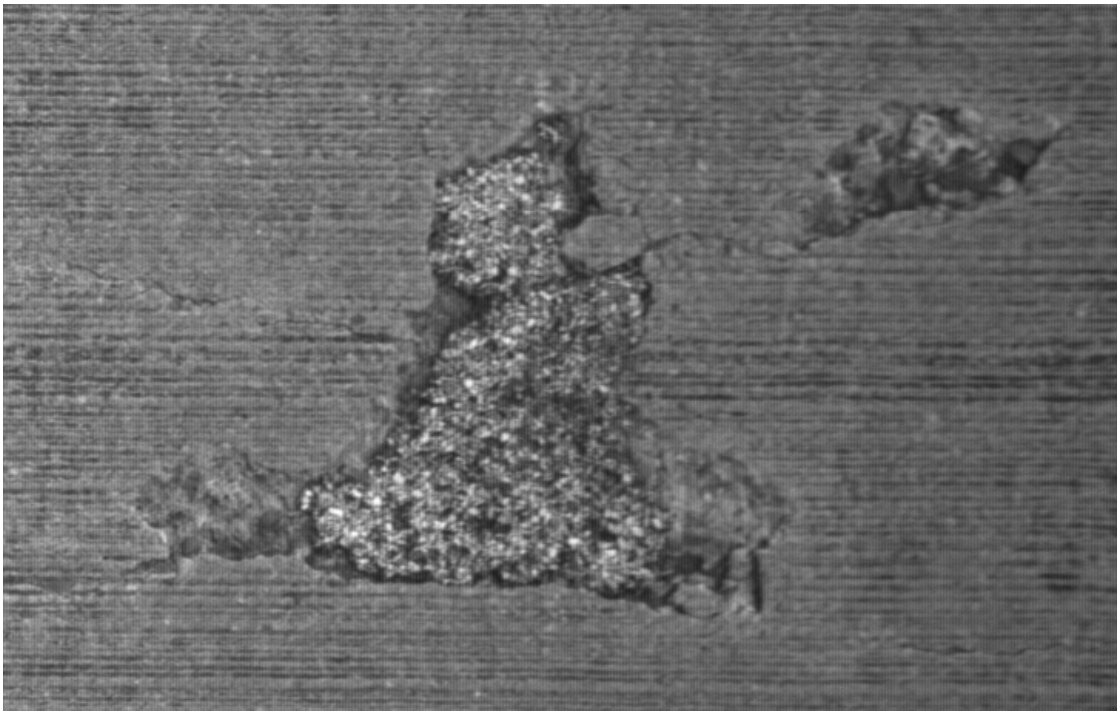

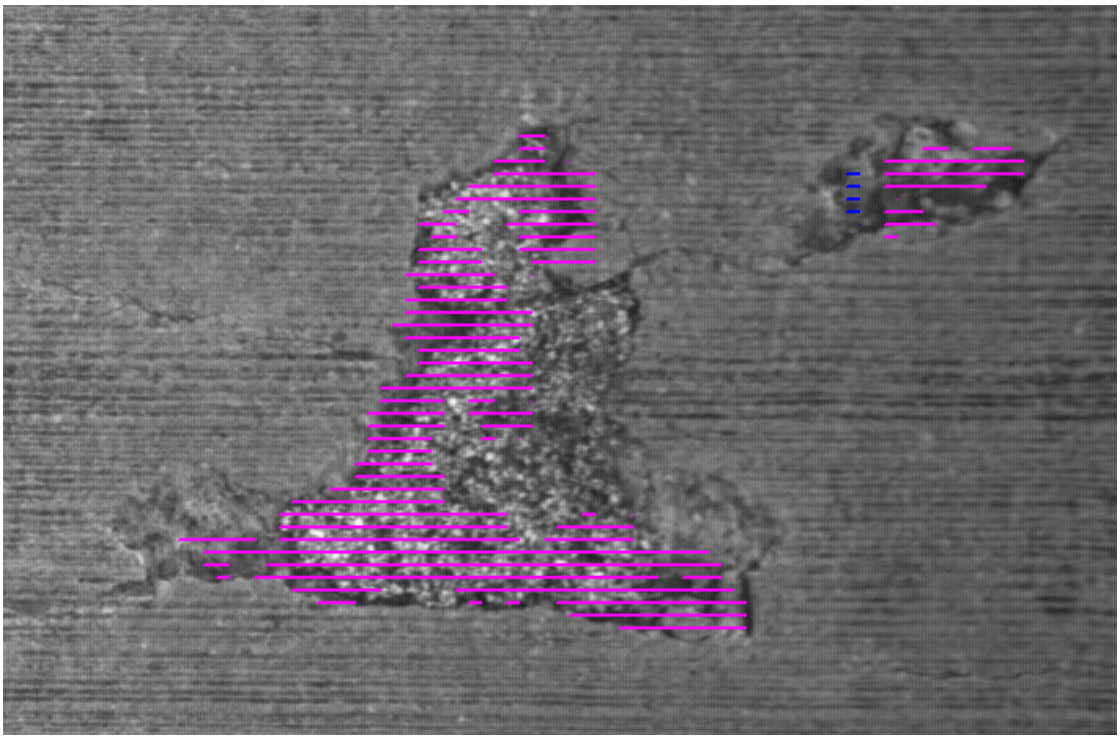

Concrete punch out cracks